Supplemental Figure 1

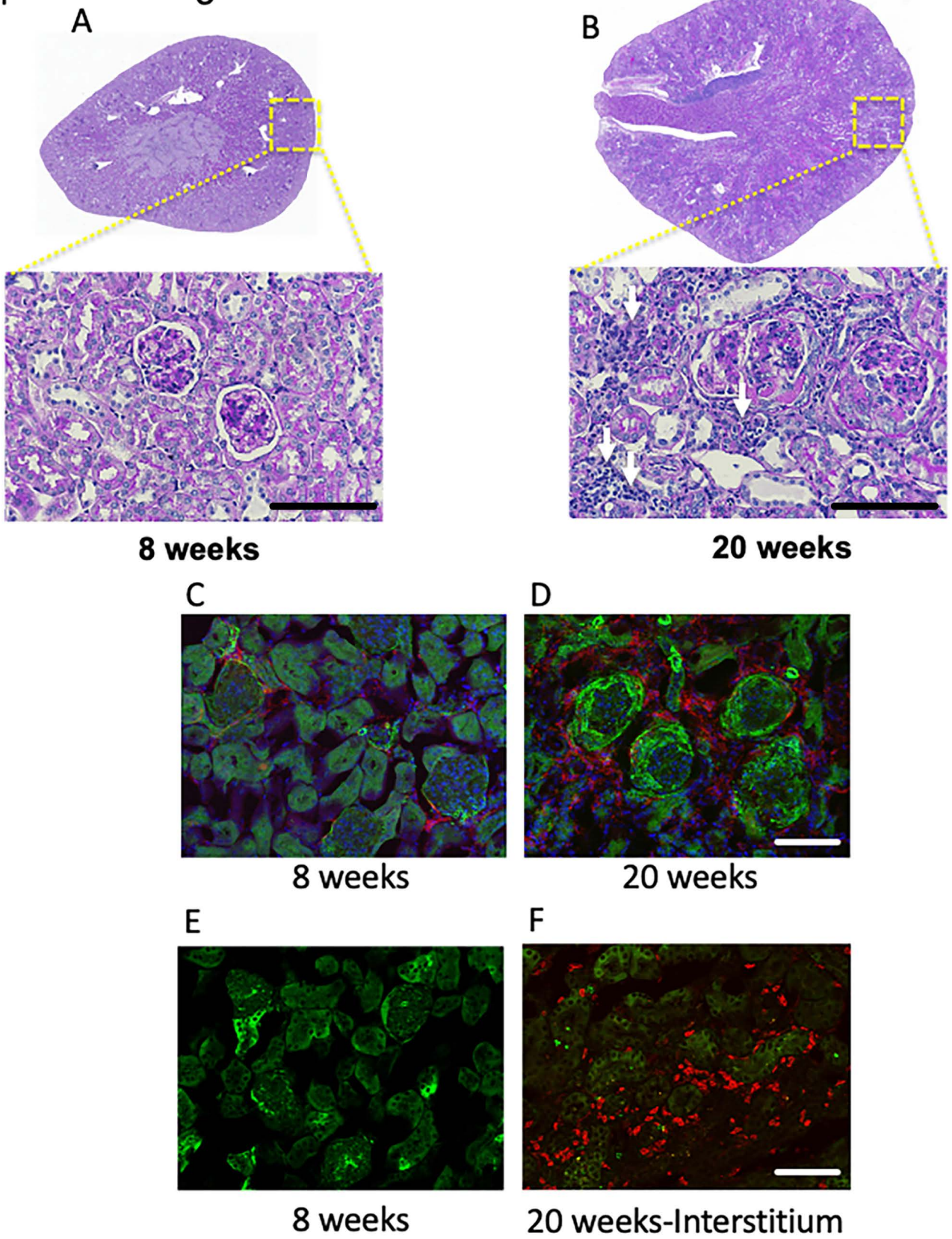

Supplemental Figure 1. Tubulointerstitial injury in lupus nephritis is accompanied by immune cell infiltration composed of macrophages and CD4 T cells

The kidneys of 8- and 20-week-old female MRL/lpr mice were analyzed by morphometry and immunofluorescence. Representative morphology by Periodic acid-Schiff (PAS)) of kidneys showed severe changes in glomeruli and tubulointerstitium with disease progression: endocapillary proliferation, infiltration of immune cells, formation of wire loops and crescents, atrophy and sclerosis is evident with age (Fig 1**A-B** and inset). White arrows point to tubulointerstitial infiltrates. At 20-weeks of age alpha smooth muscle actin positive cells are seen surrounding the glomeruli , with F4/80 positive macrophages in the periglomerular and peri-tubular regions(Fig 1**C-D**). Similarly, CD4+ T cells are seen in abundance in the periglomerular and peri-tubular regions of the nephritic kidneys (Fig 1**E-F**) Collectively this indicates that lupus nephritis is associated with severe glomerular and tubulointerstitial injury.

Supplemental Figure 2

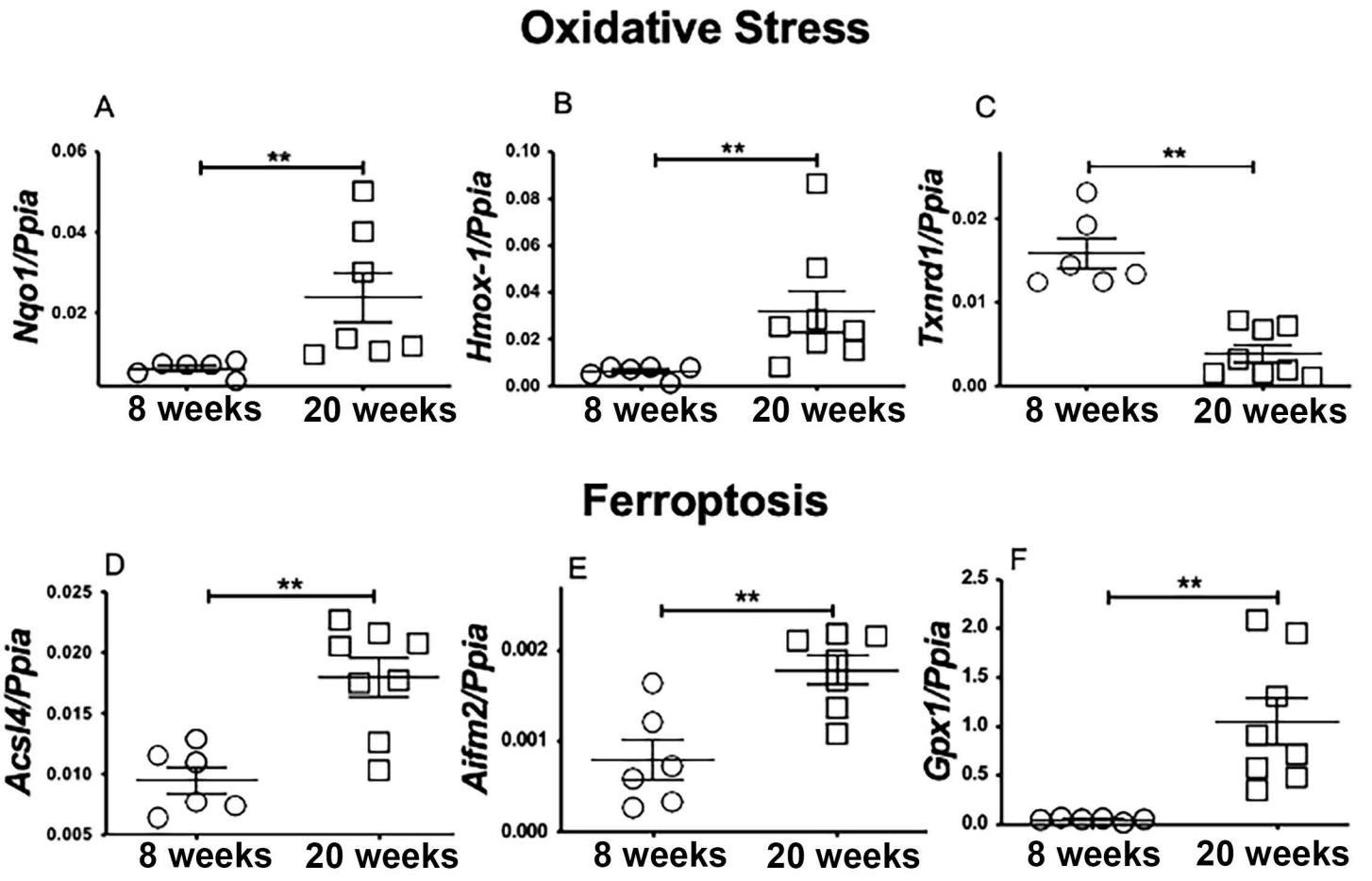

Supplemental Figure 2. Lupus nephritis kidneys display oxidative stress and a ferroptosis gene signature Compared to 8-week-old MRL/lpr females, 20-week-old nephritic females have increased oxidative stress as indicated by significantly higher gene expression of *Nqo1* **(A),** *Hmox-1* **(B)** and lower expression of *Txnrd1* **(C).** Increased iron accumulation (Figure 2) and oxidative stress in nephritic mice was associated with an increase in renal gene expression of ferroptosis markers like *Acsl4* **(D)**, *Aifm2* **(E)**, *Gpx1* **(F).** Statistical significance was determined by 2-tailed Mann-Whitney test. Data are plotted as mean ± SEM. **P < 0.001.

Supplemental Figure 3

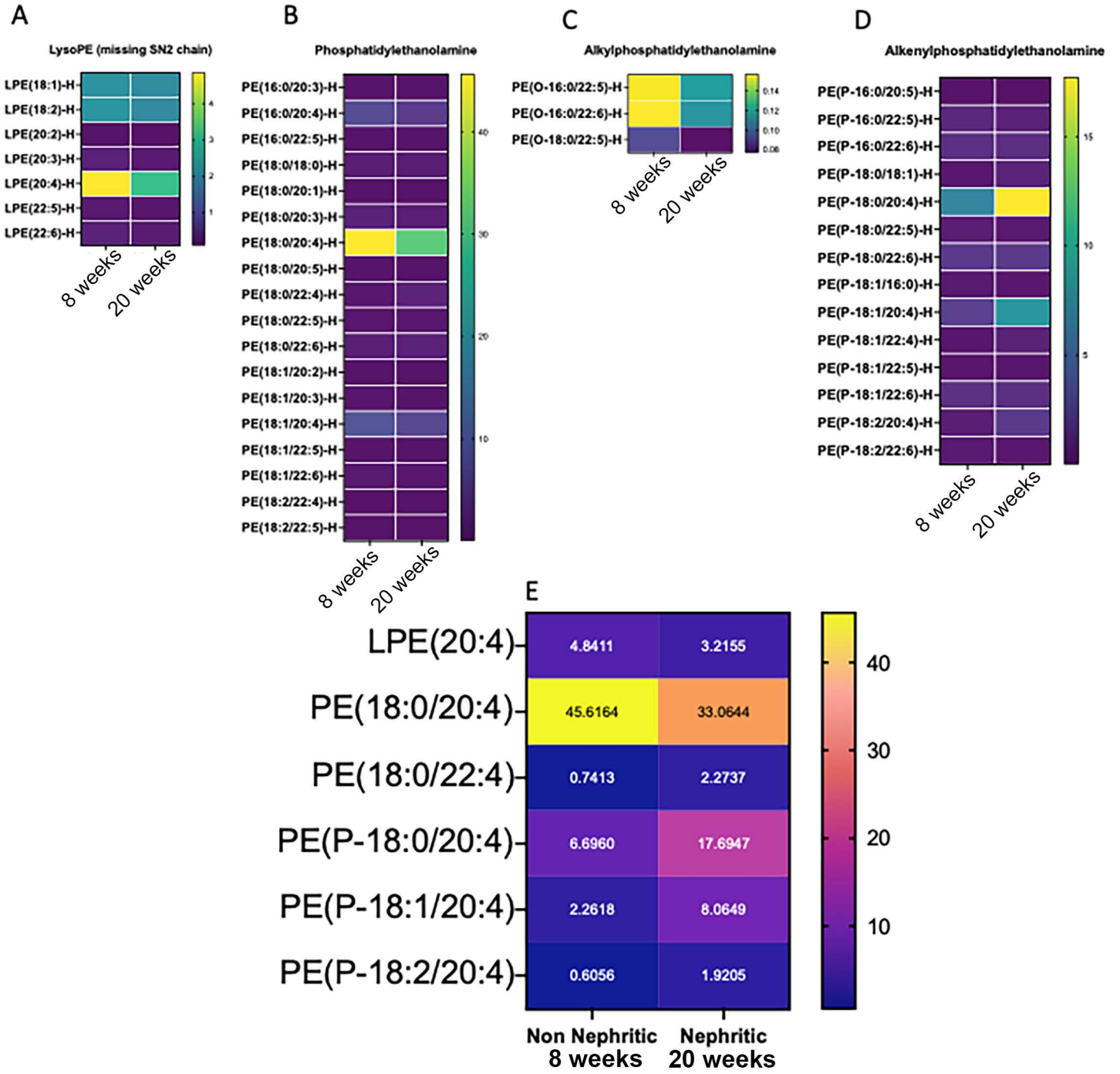

Supplemental Figure 3. Differential lipid profile in the kidneys of non nephritic (8-week-old) and nephritic (20-week-old) mice.

70-80 mg kidneys from 8-week-old (non nephritic) and 20-week-old (nephritic) MRL/lpr females were used to isolate lipids from the plasma membrane. Subsequently, the isolated lipids were subjected to semi-targeted liquid chromatography- mass spectrometry (LC-MS) to identify and quantify their lipid profile and content. Heat maps were generated by normalizing the concentration of individual lipids within each class and category to total lipid concentration within each kidney (n=6 each). Heat maps of significantly different lysophosphotidylethanolamine: LPE, phosphotidylethanolamine: PE, alkyl-phosphatidylethanolamine: PE(O) and alkenylphosphatidylethanolamine: PE(P) classes of lipids show a clear differential expression in individual lipids within and between different classes **(A-D)**. Intrarenal fingerprint obtained by averaging most differentially expressed lipids in LPE, PE, and PE(P) class in non nephritic and nephritic kidneys **(E)**. Number in each cell of E, is the lipid concentration expressed as Mean+/- SEM of 6 individual kidneys

Supplemental Figure 4

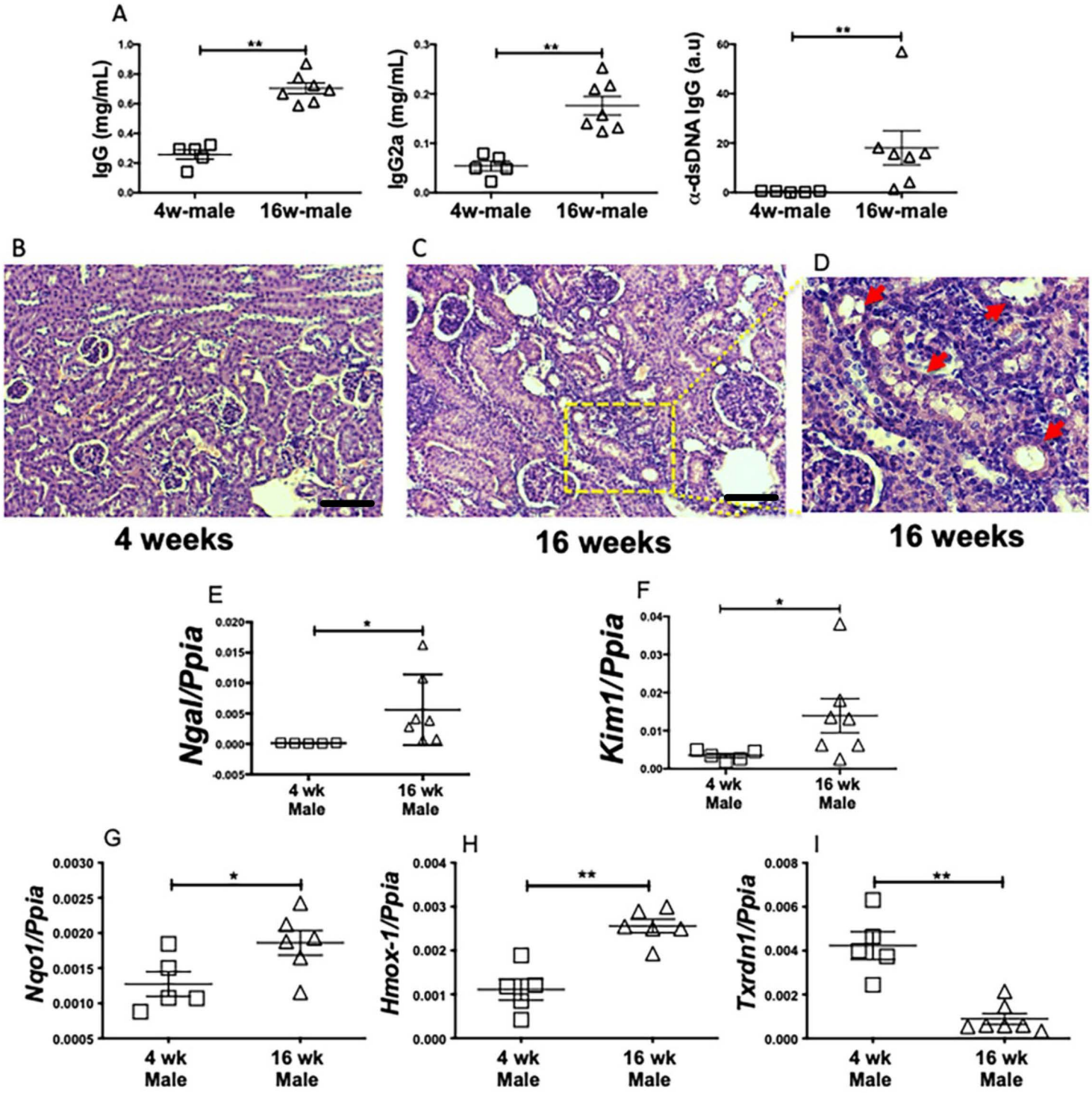

Supplemental Figure 4. Tubular injury and oxidative stress signature are a feature in a male mouse model of lupus nephritis with different etiology.
The (NZW X BXSB) F1 male mice carry two copies of TLR7 and develop progressive glomerulonephritis starting from 14 weeks of age. At 16 weeks of age, they have high titers of IgG and anti dsDNA antibodies (**A**). Compared to 4-week-old, the renal histology (H&E) of 16-week-old males shows glomerular hypertrophy, infiltration as well as injured renal tubules with dilatation, luminal debris (red arrows) (**B-D**). Scale bar = 50 μm. Representative images are shown. Proximal tubular injury markers *Ngal* (**E**) and *Kim1* (**F**), were significantly increased in 16-week-old mice. Thus, a TLR7 driven, male model of lupus also develops glomerular and tubular injury. Injury to the kidneys is associated with increased oxidative stress as indicated by an increase in *Nqo1* (**G**), *Hmox1* (**H**) and a decrease in *Txrdn1* (**I**). Statistical significance was determined by 2-tailed Mann-Whitney test. Data is presented as mean ± SEM.*P < 0.05, **P < 0.001.)

Supplemental Figure 5

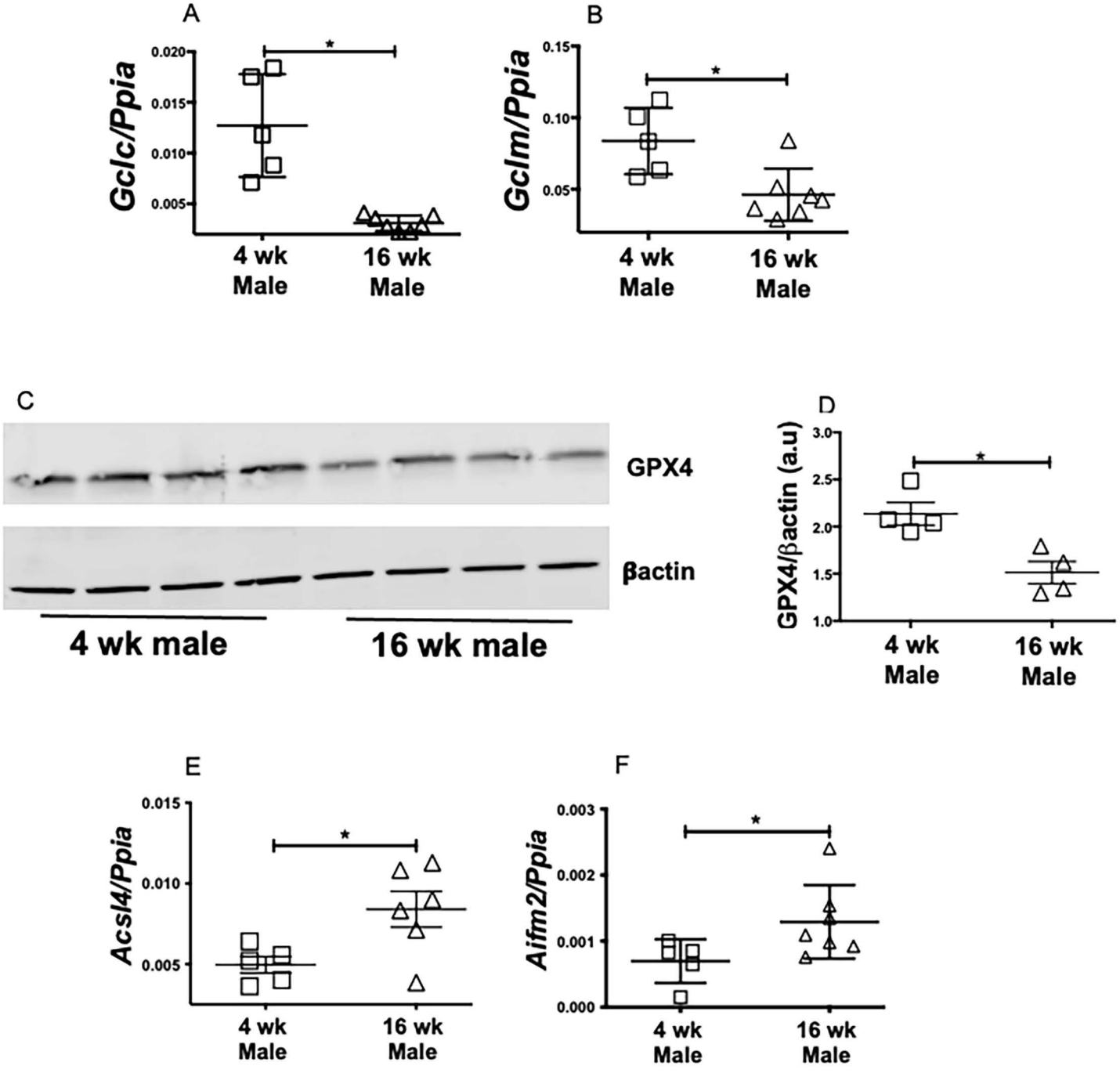

Supplemental Figure 5. Impaired glutathione biosynthesis program and ferroptosis signature in (NZW X BXSB) F1 male mice

The (NZW X BXSB) F1 male carry two copies of TLR7 and develop progressive glomerulonephritis starting from 14 weeks of age. 16-week-old nephritic males show significantly lower expression of the catalytic subunit *Gclc* (**A**) and modifier subunit *Gclm* (**B**), of glutamate cysteine ligase (GCL), the activity of which determines de novo glutathione synthesis. Compared to 4-week-old males, 16-week-old nephritic males had significantly lower expression of GPX4, the glutathione dependent ferroptosis inhibitor (**C and D**). Additionally, other markers of ferroptosis like *Acsl4* (**E**) and *Aifm2* (**F**) were also significantly elevated in 16-week-old nephritic males. Statistical significance was determined by 2-tailed Mann-Whitney test. Data are plotted as mean ± SEM. *P < 0.05. Collectively these data indicate that ferroptosis is a feature in lupus prone mice driven by different etiologies.

Supplemental Figure 6

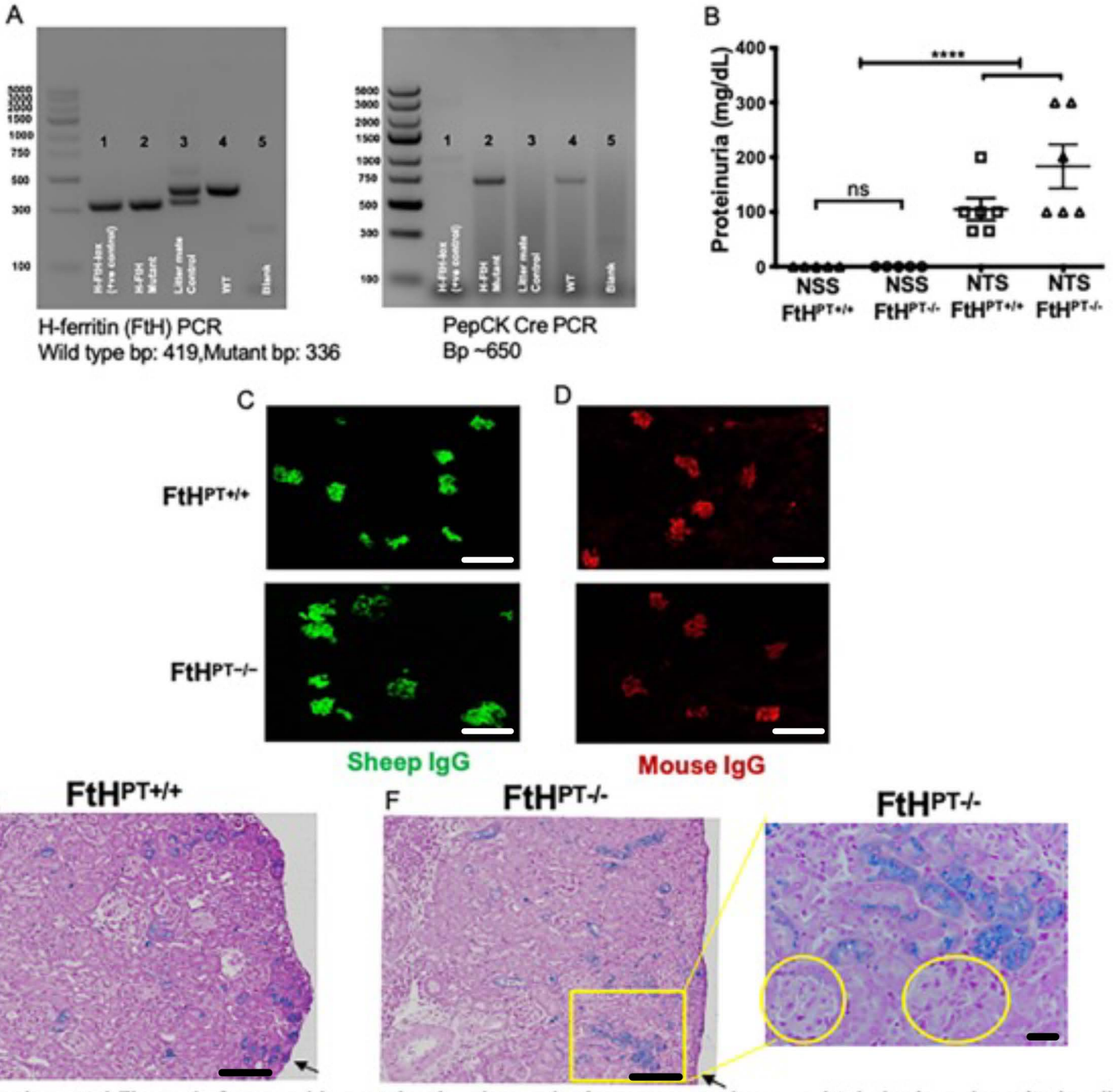

Supplemental Figure 6. Comparable proteinuria, glomerular immune complexes and tubular iron deposits in wild type mice and mice selectively deficient for FtH1 in their proximal renal tubules

The *FtH*$^{PT-/-}$ and *FtH*$^{PT+/+}$ mice used in this study were generated as described in our previous publication (PMID:24018561) and their genotype is shown (**A**). Lanes 1) FtH flox/flox (H-FtH-lox)→ positive control for loxed allele, 2) *FtH*$^{PT-/-}$ (H-FtH mutant) → Mouse deficient for FtH1 in proximal renal tubules, 3) *FtH*$^{PT+/+}$ → Litter mate control, 4) WT (Wild type) 5) Blank. 12-week-old female FtH$^{PT-/-}$ or FtH$^{PT+/+}$ (littermate controls) mice, were pre-sensitized with 100 ug sheep IgG in CFA, and four days later were injected i.v., with 100 uL **normal sheep serum (NSS) or nephrotoxic sheep serum (NTS)**. Kidneys were analyzed 14 days later. NSS did not cause any glomerulonephritis in FtH$^{PT-/-}$ or FtH$^{PT+/+}$ mice (**B**). In contract NTS caused comparable glomerular injury in both FtH$^{PT-/-}$ and FtH$^{PT+/+}$ mice as measured by proteinuria (**B**). We also observed comparable anti-sheep (heterologous) and anti-mouse (autologous) glomerular immune complex deposits (**C**) and (**D**). Similar Perls detectable iron deposits were detected in the tubular segments of FtH$^{PT+/+}$ and FtH$^{PT-/-}$ mice, whereas glomeruli (yellow circles) were devoid of observable iron deposit (**E-F and inset**). Scale bar 100 uM and 50 uM. Data was analyzed using 2-way ANOVA with pos-hoc analysis and represented as mean ± SEM. ***P < 0.0001.

Supplemental Figure 7

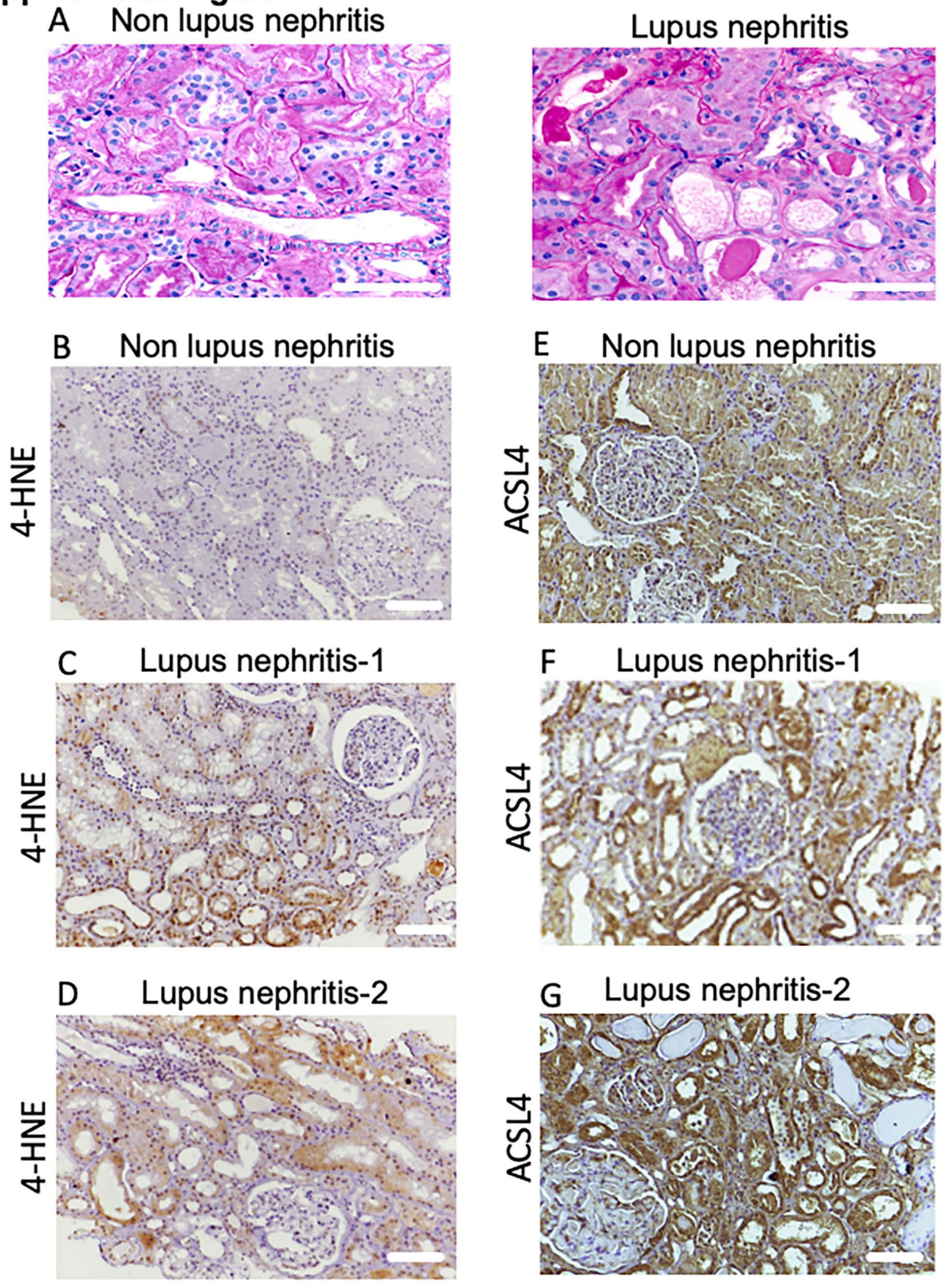

Supplemental Figure 7. Ferroptosis marker ACSL4 staining in human non-lupus and lupus nephritis kidneys . Compared to non-lupus nephritis controls, PAS-stained human biopsies from patients with class IV lupus nephritis show acute tubular injury with tubular dilatation, epithelial attenuation and casts (**A**). Non lupus patient`s kidney (B and E) and 2 individual lupus nephritis kidneys with class IV lupus nephritis were stained for 4-HNE (C-D) (lipid peroxidation marker) and ACSL4 (F-G) (ferroptosis marker). Lupus nephritis kidneys stain more intensely for 4-HNE and ACSL4. Most of the staining is in the tubular segments, the area of iron accumulation. Scale bar = 50 μm, 100 μm